

# Mapping Molecular Perturbations by a New Form of Two-Dimensional Spectroscopy

Ēriks Kupĉe<sup>†</sup> and Ray Freeman<sup>\*‡</sup>

<sup>†</sup>Agilent Technologies, 6 Mead Road, Yarnton, Oxford OX5 1QU, U.K.

<sup>‡</sup>Jesus College, Cambridge University, Cambridge CB5 8BL, U.K.

**S** Supporting Information

**ABSTRACT:** We propose a new general form of two-dimensional spectroscopy where the indirect “evolution” dimension is derived using the Radon transform. This idea is applicable to several types of spectroscopy but is illustrated here for the case of NMR spectroscopy. This “projection spectroscopy” displays characteristic correlation peaks that highlight perturbations of chemical shifts caused by temperature, pressure, solvent, molecular binding, chemical exchange, hydrogen bonding, pH variations, conformational changes, or paramagnetic agents. The results are displayed in a convenient format that allows the chemist to see all of the chemical shift perturbations at a glance and assess their rates of change and directions. As a proof of principle, we present two simple, practical examples that display two-dimensional representations of the effects of temperature and solvent on NMR spectra.

Since Jeener’s initial proposal,<sup>1</sup> the technique of two-dimensional NMR correlation spectroscopy has proved enormously useful to chemists, not least because of its clear pictorial representation of the results. We propose a new general form of this experiment in which the indirect dimension is no longer derived by the usual Fourier transformation but represents perturbations of the chemical shifts. We adopt here the Radon transform,<sup>2,3</sup> but there are examples of other possible manipulations, such as the inverse Laplace transform<sup>4–6</sup> or multivariate analysis.<sup>7</sup> The result is a simple pictorial map showing the rate at which each response in the high-resolution NMR spectrum changes as a function of temperature, pressure, solvent, molecular binding, chemical exchange, pH, conformational change, hydrogen bonding, or added lanthanide shift reagents.

We call this method “projection spectroscopy” (PROSPECT) because it employs the Radon transform to generate the indirect dimension. The Radon procedure calculates multiple line integrals along parallel beams through the experimental data and repeats the process for a set of different angles of incidence. The Radon transform  $R$  converts these line integrals into a related set of projections at right angles to the original beams:

$$R(p, \alpha) = \iint f(x) \delta(x \cos \alpha + y \sin \alpha - p) dx dy$$

where  $\delta$  is the Dirac delta function,  $p$  is the perpendicular distance of the beam from the origin, and  $\alpha$  is the angle of incidence of the beams. Whereas conventional two-dimensional spectroscopy correlates NMR frequencies in the two dimensions, projection spectroscopy charts a new kind of correlation, namely, that between chemical shifts and their rates of change caused by molecular interactions or external influences. The method belongs to a new class of experiments where the Fourier transform is replaced with some alternative manipulation. For example, the established technique known as diffusion-ordered spectroscopy<sup>8,9</sup> (DOSY) is one special case of the general concept where the diffusion dimension can be processed by the inverse Laplace transform. The new scheme is quite general and not limited to just two dimensions. Extensions to other forms of spectroscopy such as electron spin resonance and IR spectroscopy are readily imagined.

Here we deliberately restrict ourselves to two simple illustrative examples. The first maps the temperature dependence of the shifts of the different chemical sites. We call this particular application of the general idea “temperature-induced projection spectroscopy” (TIPSY). The interest lies in those situations where temperature exerts a significant effect on the chemical shifts as, for example, where OH or NH groups are involved.<sup>10</sup> After the Fourier transformation in the *direct* detection dimension, the experimental data consist of a set of one-dimensional NMR traces stacked as a function of the sample temperature; thus,  $T$  represents a new type of evolution dimension. Plotted as a two-dimensional contour map, the NMR signals form extended ridges that normally run vertically but are tilted if there is any temperature-dependent shift. Figure 1 shows a representative simulation of the evolution of the signals from three chemically shifted sites ( $a$ ,  $b$ , and  $c$ ) with different temperature dependences (assumed to be linear for simplicity).

The next stage is the Radon transform in the *evolution* dimension (here,  $T$ ), which calculates skew projections of this two-dimensional data matrix at projection angles  $\alpha = \arctan(\Delta\delta/\Delta T)$ . The projection angle is incremented in regular intervals over a range that encompasses all of the tilted ridges. (In the general case,  $\alpha$  is system-specific and not necessarily a linear function.) When the projection direction coincides with the slope of the signal ridge from site  $a$ , that particular projection acquires one sharp peak. Matching the slope of this experimental ridge has the important effect of detecting the

Received: October 12, 2012

Published: November 15, 2012

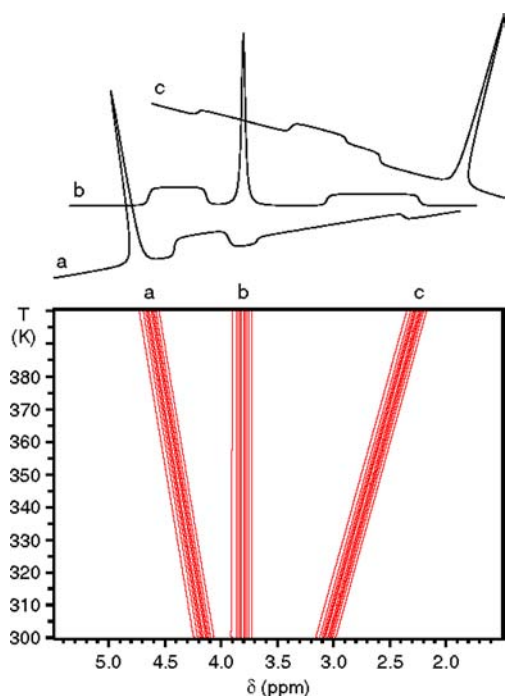


**Figure 1.** Simulated NMR responses at 600 MHz for three sites *a*, *b*, and *c* having line widths of 5 Hz and chemical shifts with different temperature coefficients ( $k_T$ ) of +2, zero, and  $-4$  Hz/K, respectively. The temperature is incremented in steps of 1 K from 300 to 400 K. Bottom: displayed as a contour map, the evolution of the NMR intensity as a function of  $T$  (vertical axis) is represented by the three extended ridges. Top: a projection at an angle aligned with one of the ridges picks up one sharp peak and two broad, flat pedestals from the other two (tilted) ridges.

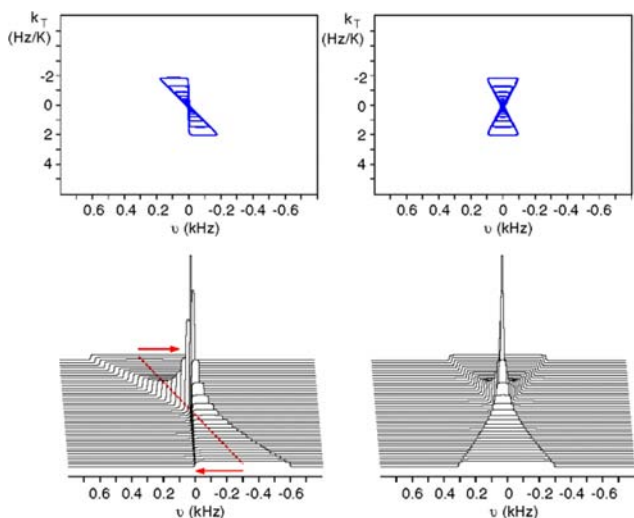


**Figure 2.** Simulations of a tilted TIPSy response (left) and the corresponding sheared response (right), represented as intensity and contour plots. The tallest peak in each of the bottom panels has been truncated at 50% height. The red line and red arrows indicate the sense of the horizontal shearing. This operation not only aligns the response parallel to the vertical axis but also brings the center of the response to the mean chemical shift on the  $\nu$  axis. The skirts of the intensity display (bottom) show how the “butterfly” shape (top) is created. It should be noted that any displacements with respect to the parent spectrum are negligible on this scale. For further simulation details, see the caption of Figure 1.

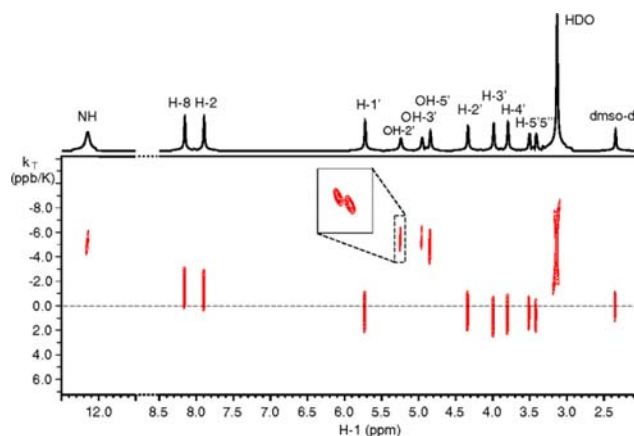


**Figure 3.** TIPSy spectrum of inosine (absolute value mode) recorded at 600 MHz, showing the chemical shift derivatives with respect to temperature ( $k_T$ , in ppb/K). The temperature was incremented from 298 to 328 K in steps of 1 K. The initial data matrix of  $31$  (real)  $\times$   $8192$  (complex) data points was expanded by two-dimensional Radon/Fourier transformation to  $128$  (real)  $\times$   $32k$  (complex) data points. The spectral widths were 24 ppb/K and 10 kHz, respectively. The power-of-two number of data points in the Radon dimension was used solely for convenience of display rather than a requirement of the transformation. The NH and OH groups show the anticipated negative temperature coefficients, together with the residual protons in HDO. The apparent distortion of the HDO line is a dynamic range effect. Very small positive displacements are observed for some aliphatic protons and comparable negative displacements for two aromatic protons. The sense of the tilt of the  $^3J(\text{HH})$  splitting from OH-2' (inset with finer digitization) indicates that this coupling decreases with temperature at  $-0.26$  Hz/K.

derivative of the chemical shift with respect to temperature. In addition to this sharp peak, there are two broad, flat responses from the tilted ridges of sites *b* and *c* (Figure 1). These broad “pedestals” have finite extents determined by the limits on the scanning range of  $\alpha$ . A complete two-dimensional array of such projections is then reassembled as horizontal traces stacked vertically as a function of  $\tan \alpha$ , representing the derivative  $k_T = \Delta\delta/\Delta T$ . Converted into a contour plot, this is the “projection spectrum”.

This projection spectrum in its raw form has two kinds of undesirable artifacts. The first of these is a characteristic tilt and displacement of each response. A maximum projected signal appears whenever  $\alpha$  is aligned with the slope of one of the extended ridges shown in Figure 1, so this tilt is transmitted to that particular response. A horizontal shearing operation can be used to compensate for these tilts (Figure 2). Shearing (actually performed in the time domain) not only corrects the tilt but also moves the center of each response to the mean value of the chemical shift measured over the frequency range under investigation.

The second artifact is the very characteristic “butterfly” shape for each response (Figure 2). As a function of the vertical offset from the center of the response, the projection picks up a broad, flat pedestal as the projection angle  $\alpha$  deviates from exact alignment with the signal ridge. This generates intensity contours with the butterfly shape, which can be visualized by consideration of the extended skirts of the intensity response illustrated in Figure 2. The butterfly shape can be converted into the more familiar four-pointed star by multiplication with a sine bell (or some other suitable windowing function) in the direct detection dimension (Figure 1S in the Supporting

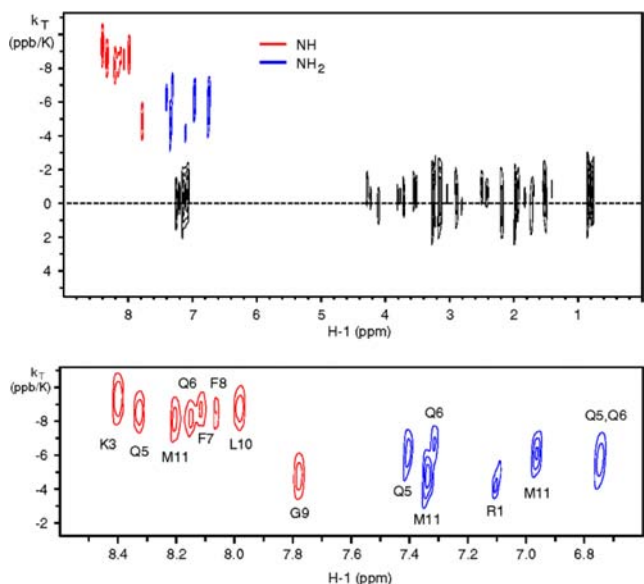


**Figure 4.** TIPSy spectrum of a 7 mM solution of substance P (Arg1-Pro2-Lys3-Pro4-Gln5-Gln6-Phe7-Phe8-Gly9-Leu10-Met11-NH<sub>2</sub>) in 9:1 H<sub>2</sub>O/D<sub>2</sub>O recorded at 600 MHz (top), showing the chemical shift derivatives with respect to temperature ( $k_T$ , in ppb/K). The temperature was incremented from 292 to 312 K in steps of 1 K. The initial data matrix of 21 (real)  $\times$  4096 (complex) data points was expanded by two-dimensional Radon/Fourier transformation to 128 (real)  $\times$  16k (complex) data points. The spectral widths were 24 ppb/K and 10 kHz, respectively. The NH (red) and NH<sub>2</sub> (blue) groups show the anticipated negative temperature coefficients. Their assignments are given in the bottom panel. The vertical scale was referenced to the H<sub>2</sub>O signal ( $-11.1$  ppb/K).<sup>11</sup> The displacements for aliphatic and aromatic protons (black) are negligible.

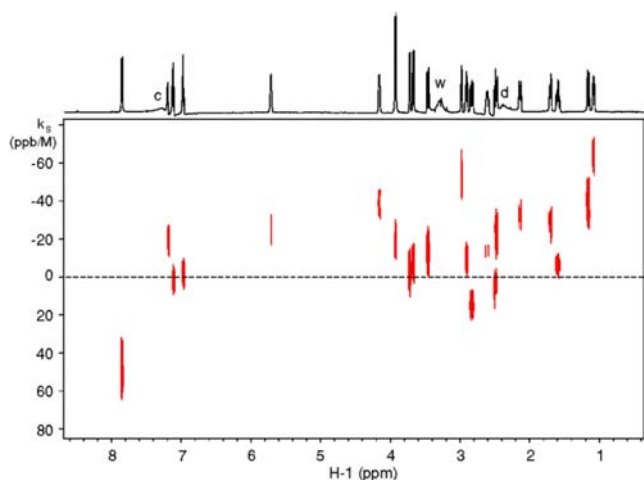


**Figure 5.** Positive and negative solvent effects ( $k_s$ , in ppm/M, where  $M$  is the molarity of CDCl<sub>3</sub>) in the 600 MHz <sup>1</sup>H NMR spectrum of a 15 mM solution of strychnine in DMSO-*d*<sub>6</sub> at 25 °C caused by gradually increasing the concentration of CDCl<sub>3</sub> from 0 to 2 M in 11 steps. The initial data matrix of 11 (real)  $\times$  8192 (complex) data points was expanded by two-dimensional Radon/Fourier transformation to 128 (real)  $\times$  32k (complex) data points. The residual proton responses from “c” (CDCl<sub>3</sub>), “w” (HDO), and “d” (DMSO-*d*<sub>6</sub>) were suppressed by a conventional postacquisition filter. It should be noted that the components of the close doublet near 2.5 ppm can be separated by their distinctly different solvent effects.

Information). Peaks in the processed projection spectrum establish the correlation between the chemical shift,  $\delta$ , of a

given site and its temperature coefficient,  $k_T = \Delta\delta/\Delta T$ . It should be noted that the multiplex advantage is preserved because signals from all of the chemical sites contribute to each projection. This offers a significant sensitivity advantage over conventional trace-by-trace measurements of perturbations in one-dimensional spectra. The form of processing outlined above was chosen with the intention of providing a clearer visualization of the Radon transform operation, but in actual practice all of the processing in the Radon domain was implemented *before* the processing in the Fourier domain (see the Supporting Information).

As the first simple experimental test of projection spectroscopy, Figure 3 shows the TIPSy spectrum of inosine in DMSO-*d*<sub>6</sub>, where the OH and NH groups show strong upfield (negative) shifts with increasing temperature due to disruption of the hydrogen bonds. The residual HDO signal from water also shows the familiar strong temperature dependence. Because the DMSO-*d*<sub>6</sub> solvent is employed as the deuterium lock signal, the lock system compensates for any temperature effect on its residual proton signal, thus defining a convenient reference point on the vertical axis. Here we assume that  $k_T \approx 0$  for DMSO-*d*<sub>6</sub>. Other solvents are known to have considerable temperature dependence (e.g.,  $k_T = -11.1$  ppb/K for H<sub>2</sub>O).<sup>11</sup> Some of the inosine aliphatic signals show a weak positive temperature effect while the aromatic protons show a weak negative effect, suggesting that any conformational changes or intermolecular interactions involving these protons are weak.

An interesting phenomenon occurs when the digital resolution is made fine enough to display the <sup>3</sup>J(HH) coupling constants. Normally,  $J$  multiplets would be oriented horizontally on this kind of chart, but the correlation response of OH-2' shows a  $J$  doublet tilted clockwise (Figure 3 inset). This occurs because this coupling constant changes with temperature, with the low-field component of the doublet increasing the apparent shift while the high-field component decreases it. The sense of the tilt establishes the fact that this coupling constant *decreases* with increasing temperature (at a rate of  $-0.26$  Hz/K); an opposite tilt would have indicated an increase in the coupling constant with temperature, as confirmed by simulations (see Figure 2S in the Supporting Information). A similar but slightly weaker effect is evident in the OH-3' response (not shown) but is essentially zero in the OH-5' response (not shown).

A further example of two-dimensional TIPSy spectroscopy is shown in Figure 4 for the case of a small peptide, substance P (11 amino acid residues). This neuropeptide of the tachykinin family is of interest because it is believed to be involved in a wide range of physiological processes, including pain transmission, inflammation, blood flow, salivation, and muscle contraction.<sup>12</sup> It should be noted that the signal from Arg-1 (blue), which is normally concealed within a crowded region of the spectrum, is clearly revealed by the two-dimensional TIPSy experiment. The reduced temperature effect of the Gly-9 NH proton is indicative of intramolecular hydrogen-bond formation.<sup>10,12</sup>

Solvent effects have been well-studied by high-resolution NMR in an attempt to understand the nature of molecular interactions. As a second practical illustration of projection spectroscopy, we show the effect on the proton NMR spectrum of strychnine (600 MHz at 25 °C) when a 0.5% solution in DMSO-*d*<sub>6</sub> is gradually diluted by the addition of small amounts of CDCl<sub>3</sub> (Figure 5). The progressive change of the solvent causes both positive and negative chemical shift variations. The

components of a close doublet (near 2.5 ppm) can be separated and tentatively assigned according to their distinctly different solvent effects. A detailed analysis of the results in terms of specific molecular interactions is beyond the scope of this article, but a profound effect on the proton chemical shifts is obvious.

Two-dimensional projection spectroscopy (PROSPECT) using the Radon transform offers a clear pictorial representation of measurements that could have been made by more conventional experiments, but this new “fingerprint” mode of display should commend itself to the practical chemist because it highlights *change*. It allows any perturbations of chemical shifts to be viewed at a glance and their rates of change and directions to be evaluated, replacing tedious lists of numbers. Many interesting types of molecular interactions could be explored in this manner—molecular binding studies and drug design are examples that spring to mind. The method is quite general and is not restricted to NMR spectroscopy or to just two dimensions.

## ■ ASSOCIATED CONTENT

### ● Supporting Information

Line shape transformation upon sine-bell window multiplication, simulation of temperature effects on the multiplet structure in the 2D TIPSy spectra, and further processing details. This material is available free of charge via the Internet at <http://pubs.acs.org>.

## ■ AUTHOR INFORMATION

### Corresponding Author

rf110@hermes.cam.ac.uk

### Notes

The authors declare no competing financial interest.

## ■ REFERENCES

- (1) Jeener, J. Presented at the Ampere International Summer School, Basko Polje, Yugoslavia, 1971.
- (2) Deans, S. R. *The Radon Transform and Some of Its Applications*; Wiley: New York, 1992.
- (3) Kupče, Ě.; Freeman, R. *Concepts Magn. Reson.* **2004**, *22A*, 4–11.
- (4) Deakin, M. A. B. *Arch. Hist. Exact Sci.* **1981**, *25*, 343–390.
- (5) Provencher, S. W. *Comput. Phys. Commun.* **1982**, *27*, 213–227.
- (6) Callaghan, P. T.; Arns, C. H.; Galvosas, P.; Hunter, M. W.; Qiao, Y.; Washburn, K. E. *Magn. Reson. Imaging* **2007**, *25*, 441–444.
- (7) Windig, W.; Antalek, B. *Chemom. Intell. Lab. Syst.* **1997**, *37*, 241–254.
- (8) Morris, K. F.; Johnson, C. S., Jr. *J. Am. Chem. Soc.* **1993**, *115*, 4291–4299.
- (9) Morris, G. A. Diffusion-Ordered Spectroscopy. In *Encyclopedia of Magnetic Resonance*; Harris, R. K., Wasylshen, R. E., Eds.; Wiley: Chichester, U.K., 2009.
- (10) Baxter, N. J.; Williamson, M. P. *J. Biomol. NMR* **1997**, *9*, 359–369.
- (11) Gottlieb, H. E.; Kotlyar, V.; Nudelman, A. *J. Org. Chem.* **1997**, *62*, 7512–7515.
- (12) Baek, S. B.; Lim, S. C.; Lee, H. J.; Lee, H. C.; Kim, C. *Bull. Korean Chem. Soc.* **2011**, *32*, 3702–3706.